Characteristic features of Auger spectra from adatoms on metals

N. Bonini,[1,2] M. I. Trioni,[2] and G. P. Brivio[1,2]
[1]*Dipartimento di Scienza dei Materiali, Università di Milano–Bicocca, Via Cozzi 53, 20125 Milano, Italy*
[2]*Istituto Nazionale per la Fisica della Materia, UdR Milano Bicocca, via Cozzi 53, 20125 Milano, Italy*
(Received 5 December 2000; revised manuscript received 20 March 2001; published 28 June 2001)

In this work we perform a full *ab initio* density-functional theory calculation, within the embedding method, of the Auger spectra of atomic impurities both inside a metal bulk and just inside the solid surface and chemisorbed on it. We consider a Na atom on and in a jellium-Ag host. In particular, the Auger spectra of the electronic transitions KL_1V and $KL_{2,3}V$ (core-core-valence) are worked out. The calculated profiles display features which are different for the same atom adsorbed on a metal and inside the same bulk material. Such specific features could help identifying the contribution to the measured Auger signal only due to adsorbates.

DOI: 10.1103/PhysRevB.64.035424 PACS number(s): 68.43.−h, 82.80.Pv, 32.80.Hd, 71.15.Mb

I. INTRODUCTION

The fact that Auger spectroscopy could provide valuable information about local electronic structures is well established,[1,2] since several experimental and theoretical works on simple metals[3–5] and alloys[6–9] have shown that the Auger profile allows one to gain insight into the nature of the distortion of the local density of states around an ionized core site. Because of the sensitivity of this quantity to the local environment, it follows that an Auger line related to a given transition recorded by electron spectroscopy may comprise several contributions appearing as a consequence of differences in the electronic properties of bulk and near-surface regions. However, the possibility that surface effects may appear is strongly related to the energy of the Auger electron: when the energies are of the order of 100 eV the electron mean free path is quite short and one would expect surface effects to manifest themselves; on the other hand, at higher energies the escape depth is larger and the contribution to the Auger spectra is mainly from the bulk.

The technique of the Auger photoelectron coincidence spectroscopy (APECS) could be a useful tool to directly select and study the Auger decay at distinct sites in a sample, since it takes advantage of the temporal relationship between the photoelectron and the Auger electron emitted from a single excitation event and exploits the core-level shift from inequivalent sites in a crystal.[10,11] So far the APECS has revealed correlation features hidden in the standard Auger and photoemission spectra,[11] but recent improvements in the count rates are expected to allow for the measurement of electronic structures characteristic of adsorption.

Though it is now possible to probe and investigate the Auger emission from surface regions, there are only very few *ab initio* theoretical calculations that go beyond the bulk approximation, including surface effects.[12–14] In bulk calculations the decaying atom is inside the solid and the created Auger electrons are implicitly taken as a measure of the experimentally observed spectrum. To go beyond this approximation it is necessary to calculate losses and scattering processes involving Auger electrons, and to consider decays of atoms near the surface.

In the present work we shall confine ourselves to the no-loss part of unscattered Auger electrons and we shall only deal with the effect of different electronic environments on the Auger transition probabilities. We perform a full *ab initio* calculation, within the density-functional theory framework in the local-density approximation, of the core-core-valence (CCV) KLV Auger transition rates of an atomic impurity located inside a metal bulk and, for the first time (to our knowledge), both just inside the solid and chemisorbed on it. In particular, the Auger spectra from the CCV electronic transitions KL_1V and $KL_{2,3}V$ are worked out for Na in and on an Ag (jelliumlike) host. We observe that in general the Auger decay dominates the deexcitation process of light atoms such as Na, when a core hole is created in the K shell. In this case both KLL and KLV Auger processes are possible. We concentrate on the latter ones since the emission line may be significantly affected by the interaction with the host electrons. We also recall that there are several experimental and theoretical investigations of Auger spectra of Na,[3,4,15,16] and that Ag is a suitable host for a Na impurity, which also chemisorbs on this surface without diffusing into the bulk. It is worth noting that the jellium model is not able to account for the Ag d band which could, as proposed in Ref. 6 for Mg-Ag alloys, influence the Auger line shape of the impurity. We also observe that our approach is based upon the single-particle approximation so that many-body effects such as shake-up satellites are not treated. Such many-body features which are more important for core-valence-valence (CVV) transitions can be taken into account by phenomenological models explicitly considering a continuum substrate[17] or by multiconfigurational interaction.

In Sec. II we present the theoretical approach describing the main assumptions of our one-electron calculation. Section III illustrates the calculated KLV Auger profiles of the impurity in three different positions with respect to the substrate. The results display different characteristic features according to the location of the atom. Finally the last section is devoted to conclusions and discussion.

II. THEORETICAL FRAMEWORK

Our theoretical treatment of the core-core-valence (CCV) Auger process of an atom in and on a metal host is based on a two-step model, in which the Auger decay is independent of the creation of the initial core hole. We assume that when

the Auger event takes place, the electrons refer to a relaxed quasi-ground-state corresponding to an effective potential with a core hole present.[4,17] We treat such systems solving the Kohn and Sham (KS) equation of the density-functional theory (DFT) in the local-density approximation (LDA) by the Green-function embedding approach.[18,19] The KS equation is expanded on a linear augmented plane-wave LAPW basis set and an all-electron calculation is performed for the impurity.[20] We recall that our approach is able to account for a single isolated impurity so that our results are to be considered as a low-density limit. However, we expect excited-state spectra to be mainly influenced for a certain atom on a specific substrate by local geometry more than by impurity-impurity interactions. But the advantage of the Green-function method compared to others, such as the supercell geometry, is that it can deal with a true continuum spectrum such as the valence band of the metal, whose description is fundamental for the understanding of the Auger profiles.

The transition-matrix elements describing the Auger process are calculated by the Slater determinant formed by the eigenstates solution of the KS single-particle equation as initial and final states. In the KS equation the effective potential includes the potential of a self-consistently screened $1s$ core hole. Though in a *KLV* Auger transition the initial- and final-state core holes are different, we consider the two core holes to have the same effect on valence electrons.[21] This is an accurate approximation since we have checked that distinct core holes affect the local density of states very little.[4] To calculate the Auger transition probability from the matrix elements we use the Fermi golden rule, extending the approach in Ref. 5 for an impurity in bulk jellium. In fact, the lower symmetry of an atom-surface system breaks the spherical symmetry of the previous configuration.

We now present the main equations of our treatment, starting with the Auger transition probability $P(E)$ for an electron emitted with kinetic energy E (atomic units are used hereafter),

$$P(E)=2\pi\sum_{A,v}\sum_{m_{c_f},\sigma_{c_f}}\frac{1}{2}\frac{1}{2l_{c_i}+1}\times\sum_{m_{c_i},\sigma_{c_i}}|\mathrm{D}_{A,c_i,c_f,v}-\mathrm{E}_{A,c_i,c_f,v}|^2\times\delta(E+E_{c_i}-E_{c_f}-E_v),\tag{1}$$

where A, c_i, c_f, v represent the Auger, the initial- and final-state core hole, and the valence electron, respectively. In Eq. (1), the direct $D_{A,c_i,c_f,v}$ and exchange $E_{A,c_i,c_f,v}$ matrix elements are given by

$$\mathrm{D}_{A,c_i,c_f,v}=\int d\mathbf{r}_1 d\mathbf{r}_2\psi^*_{c_f}(\mathbf{r}_1)\psi_{c_i}(\mathbf{r}_1)\frac{1}{|\mathbf{r}_1-\mathbf{r}_2|}\psi^*_v(\mathbf{r}_2)\psi_A(\mathbf{r}_2)\tag{2}$$

and

$$\mathrm{E}_{A,c_i,c_f,v}=\int d\mathbf{r}_1 d\mathbf{r}_2\psi^*_{c_f}(\mathbf{r}_1)\psi_A(\mathbf{r}_1)\frac{1}{|\mathbf{r}_1-\mathbf{r}_2|}\psi^*_v(\mathbf{r}_2)\psi_{c_i}(\mathbf{r}_2).\tag{3}$$

In Eq. (1) we have averaged over the magnetic quantum number m_{c_i} and the spin σ_{c_i} of the decaying hole and summed over the other states involved in the transition. The core wave functions of the atom are

$$\psi_c(\mathbf{r})=R_{l_c}(E_c,r)Y_{l_c,m_c}(\Omega)\chi(\sigma_c),\tag{4}$$

where $Y_{l,m}(\Omega)$ are spherical harmonics and $\chi(\sigma)$ denote the spin states. The radial part, $R_{l_c}(E_c,r)$, of these wave functions is evaluated solving the semirelativistic[22] Schrödinger equation self-consistently. The Auger-electron wave function has the following partial-wave expansion:

$$\psi_A(\mathbf{r})=\sum_l\sum_{m=-l}^{l}R_l(k_A,r)Y_{l,m}(\Omega)Y^*_{l,m}(\hat{k}_A)\chi(\sigma_A).\tag{5}$$

As CCV transitions produce rather high-energy Auger electrons, the dispersion relationship of the Auger electron with wave vector $\mathbf{k}_A$ is taken as a free particle one $E=k_A^2/2$. In Eq. (5) $R_l(k_A,r)$ is the solution of the radial semirelativistic Schrödinger equation up to the Wigner-Seitz radius, matched outside it with a free-electron wave function (energy normalization is used).[4,5] The energy of the Auger electron is determined by the δ function in Eq. (1) (see also the discussion in Sec. III).

In the calculation of the transition probability in Eq. (1) we have to evaluate products of valence-electron wave functions times the energy conservation δ of Dirac, and sum over the continuum of all valence states. This can be easily done exploiting the following relationship with the Green function $G(\mathbf{r},\mathbf{r}';E)$ of the system[23] (hereafter $E=E'+i\delta$, with E' the energy belonging to the continuous spectrum of the system and δ a positive, infinitesimal quantity)

$$\sum_v\delta(E-E_v)\psi_v(\mathbf{r})\psi^*_v(\mathbf{r}')=\frac{1}{2\pi i}[G(\mathbf{r},\mathbf{r}';E)-G^*(\mathbf{r}',\mathbf{r};E)].\tag{6}$$

Direct use of the Green function naturally accounts for the continuous distribution of the valence electronic states. Integrating in a volume V Eq. (6) for $\mathbf{r}=\mathbf{r}'$, one obtains the local density of states (LDOS)

$$\rho_V(E)=\frac{1}{\pi}\int_V d\mathbf{r}\,\mathrm{Im}G(\mathbf{r},\mathbf{r};E).\tag{7}$$

In our calculation we expand the Green function on a LAPW basis set[20]

$$G(\mathbf{r},\mathbf{r}';E)=\sum_{n,L}\sum_{n',L'}\mathcal{G}_{n,n',L,L'}(E)f_{n,l}(\mathbf{r})f_{n',l'}(\mathbf{r}')Y_L(\Omega)Y^*_{L'}(\Omega'),\tag{8}$$

where $L=l,m$ and $f_{n,l}(\mathbf{r})$ are real.

We proceed by summing over spins (we neglect spin-orbit coupling) and integrating on $\hat{k}_A$ over a full solid angle, since in the present work we are not interested in angle-resolved Auger emission. Hence, for KL_1V transitions, which correspond to $l_{c_i}=l_{c_f}=0$, we find

$$P_{KL_1V}(E)=2\sum_{n,n'}\sum_{L}\Delta\mathcal{G}_{n,n',L,L}(E+E_{c_i}-E_{c_f})\times\left[\mathcal{D}_{0,n}(l,0,0,l;E)\mathcal{D}_{0,n'}(l,0,0,l;E)+\frac{1}{(2l+1)^2}\times\mathcal{E}_{l,n'}(l,0,0,l;E)\mathcal{E}_{l,n}(l,0,0,l;E)\right]-\frac{\mathrm{Re}[\Delta\mathcal{G}_{n,n',L,L}(E+E_{c_i}-E_{c_f})]}{2l+1}\times\mathcal{D}_{0,n'}(l,0,0,l;E)\mathcal{E}_{l,n}(l,0,0,l;E), \tag{9}$$

and for $KL_{2,3}V$ transitions, where $l_{c_i}=0$ and $l_{c_f}=1$, we obtain

$$P_{KL_{2,3}V}(E)=8\pi\sum_{n,n'}\sum_{L,L'}\sum_{L_A}\sum_{m_{c_f}=-1}^{1}C^{*}_{1,m_{c_f},L',L_A}C_{1,m_{c_f},L,L_A}\times\left\{\Delta\mathcal{G}n,n',L,L'(E+E_{c_i}-E_{c_f})\times\left[\frac{1}{9}\mathcal{D}_{1,n'}(l_A,0,1,l';E)\mathcal{D}_{1,n}(l_A,0,1,l;E)+\frac{1}{(2l+1)(2l'+1)}\times\mathcal{E}_{l',n'}(l_A,0,1,l';E)\mathcal{E}_{l,n}(l_A,0,1,l;E)\right]-\frac{\mathrm{Re}[\Delta\mathcal{G}_{n,n',L,L'}(E+E_{c_i}-E_{c_f})]}{3(2l+1)}\times\mathcal{D}_{1,n'}(l_A,0,1,l';E)\mathcal{E}_{l,n}(l_A,0,1,l;E)\right\}, \tag{10}$$

where

$$\Delta\mathcal{G}_{n,n',L,L'}(E)=\frac{1}{2i}[\mathcal{G}_{n,n',L,L'}(E)-\mathcal{G}^{*}_{n',n,L',L}(E)], \tag{11}$$

$$C_{L,L_1,L_2}=\int d\Omega Y_L(\Omega)Y_{L_1}(\Omega)Y^{*}_{L_2}(\Omega), \tag{12}$$

$$\mathcal{D}_{k,n}(l_A,l_{c_i},l_{c_f},l;E)=\int r^2dr\int r'^2dr'R_{l_{c_f}}(E_{c_f},r)\times R_{l_{c_i}}(E_{c_i},r)\frac{r^k_<}{r^{k+1}_>}f_{n,l}(r')R_{l_A}(k_A,r'), \tag{13}$$

$$\mathcal{E}_{k,n}(l_A,l_{c_i},l_{c_f},l;E)=\int r^2dr\int r'^2dr'R_{l_{c_f}}(E_{c_f},r)\times R_{l_A}(k_A,r)\frac{r^k_<}{r^{k+1}_>}f_{n,l}(r')R_{l_{c_i}}(E_{c_i},r'). \tag{14}$$

It is worth noting that the expressions given in Eqs. (9) and (10) reduce to those in Ref. 5 in the case of a spherically symmetric system. In such a case one exploits the property that the Green-function expansion coefficients are symmetric,[24] i.e., $\Delta\mathcal{G}_{n,n',L,L'}=\mathrm{Im}\mathcal{G}_{n,n',L,L'}$, and by observing that they are diagonal in L and independent of m, one can write $\mathcal{G}_{n,n',l}\delta_{l,l'}\delta_{m,m'}$ in Eq. (8). Finally, we stress that our approach allows one to obtain both bulk and surface results consistently using the same approximations. This is necessary to assess the importance of surface effects.

III. RESULTS

First, in order to test our model and to make a comparison with previous works, we performed bulk calculations on two widely studied simple metals, i.e., Na and Mg.[3–5] Our theoretical results for KL_1V and $KL_{2,3}V$ Auger transitions on such systems show a quite satisfactory agreement with the experimental results shown in Refs. 3–5. Such agreement confirms that our simple model, which neglects band-structure effects, is able to take into account the main features of KLV Auger profiles. We have also checked that our calculated results for Mg in Mg bulk reproduce exactly those of Ref. 5 because, as already stressed, our method reduces to that in Ref. 5 for an impurity in bulk.

We now present the results for a Na atom interacting with an Ag host with different geometries of the system, namely we consider the impurity in bulk, just inside the metal at $z=-2.0a_0$ (a_0 is the Bohr radius) and chemisorbed on the surface at $z=2.5a_0$ (the direction of the z axis is normal to the positive background edge at $z=0$, and points outside jellium). The Ag substrate is described by a jellium with charge density $\rho_b=3/(4\pi r_s^3)$ where $r_s=3.02a_0$. In our calculations we use an embedding sphere of radius $r_{emb}=7a_0$, a muffin-tin of radius $r_{MT}=2.8a_0$, while the LDA exchange-correlation functional is that of Ceperly and Alder.[25] The cutoff energy for the basis functions in the interstitial region is 22 Ry, and the maximum angular momentum for the Green-function expansion, $l_{\max}$, is chosen as 8. The integrals in Eqs. (13) and (14) should, in principle, be evaluated over the whole space. Nevertheless, we perform the integrals up to the radius of the embedding sphere. This

is a good approximation because in the exchange term [Eq. (14)] the localized core wave functions limit the range of both integrations, while for the direct term [Eq. (13)] we have checked that the integral reaches a constant value for an integration radius much less than r_{emb}, essentially because of the strong orthogonality between the valence and Auger wave functions.

As already shown for atoms in metal bulk,[5,9] our model is able to well account for the line shape of CCV Auger transitions, but we expect that our calculations of the Auger electron kinetic energy will not agree with experiment. This is because the LDA generally underestimates the binding energy of atomic core-hole states and Koopmans's theorem, which we use to evaluate the kinetic energy of the Auger electron, is known to neglect any electronic relaxation processes.

In Figs. 1, 2, and 3 we show the LDOS [panels (a)] and the core-ionized LDOS [panels (b)], the KL_1V transition rates [panels (c)], and $KL_{2,3}V$ transition rates [panels (d)] of the Auger decay, for a Na atom in Ag bulk, at $z=-2.0a_0$, and at $z=2.5a_0$ from the Ag surface. The LDOS's are calculated using Eq. (7) and performing the spatial integral in a sphere of radius $r_s=3.02a_0$ around the impurity. In fact it is in such a volume that the properties of the valence-electron wave functions essentially affect the Auger transitions since, as we have checked, the matrix elements in Eqs. (13) and (14) are negligible outside this sphere. The Auger transition rates are calculated using Eqs. (9) and (10) and the energies of the Auger electrons are shifted so that the top of the emission band is at the Fermi edge.

We describe first the case of Na in Ag bulk. The LDOS in Fig. 1(a) shows the characteristic square-root behavior of a free-electron metal. This result is the expected one if we consider such a system in term of the equivalent cores approximation[7] since the difference in local charge between the host and the Na impurity, ΔZ, is 0. The comparison between Fig. 1(a) and Fig. 1(b) shows that the presence of a core hole in the impurity atom drastically changes the shape of the LDOS around Na. We find that the core hole causes a significant localization of the *s* electrons near the bottom of the valence band and an increase of the LDOS of the *p* electrons. This distortion is what we expect since ΔZ changes from 0 to +1 after core ionization,[7] and is in agreement with the result of previous studies on simple bulk metals.[4,5] The calculated KL_1V [Fig. 1(c)] and $KL_{2,3}V$ [Fig. 1(d)] Auger transition rates closely resemble the shape of the LDOS around core-ionized impurity and the difference between the two spectra is a consequence of distinct matrix elements. The results for Na at $z=-2.0a_0$ display other new features with respect to the same impurity in bulk. The bump at low energy in the LDOS [Fig. 2(a)] is essentially due to the contribution of sodium 3*s* resonance. Such a resonance, which is absent for Na in Ag bulk, arises here because the presence of the surface reduces the symmetry of the system. After the removal of an electron from the core, the attractive electrostatic potential created by the hole shifts this peak to lower energies [Fig. 2(b)] compared to that in Fig. 2(a). The decrease in the density of metal states seen by this resonance as it moves towards the bottom of the metal band yields a narrowing of the corresponding peak in LDOS. The Auger transition rates in Figs. 2(c) and 2(d) clearly reflect the distortion of the LDOS due to the presence of a core hole. In Fig. 3 we report the results for Na at $z=2.5a_0$. We observe that the Na 3*s* resonance is peaked much above the Fermi energy and hence only partially occupied in the LDOS in Fig. 3(a). Thus the main effect in the bond formation is the charge transfer of the Na 3*s* electron towards the metal surface. When an electron is removed from the core, the attractive potential created by the hole lowers this resonance below the Fermi energy yielding an almost complete occupation of this level [Fig. 3(b)]. The charge that occupies this resonance is essen-

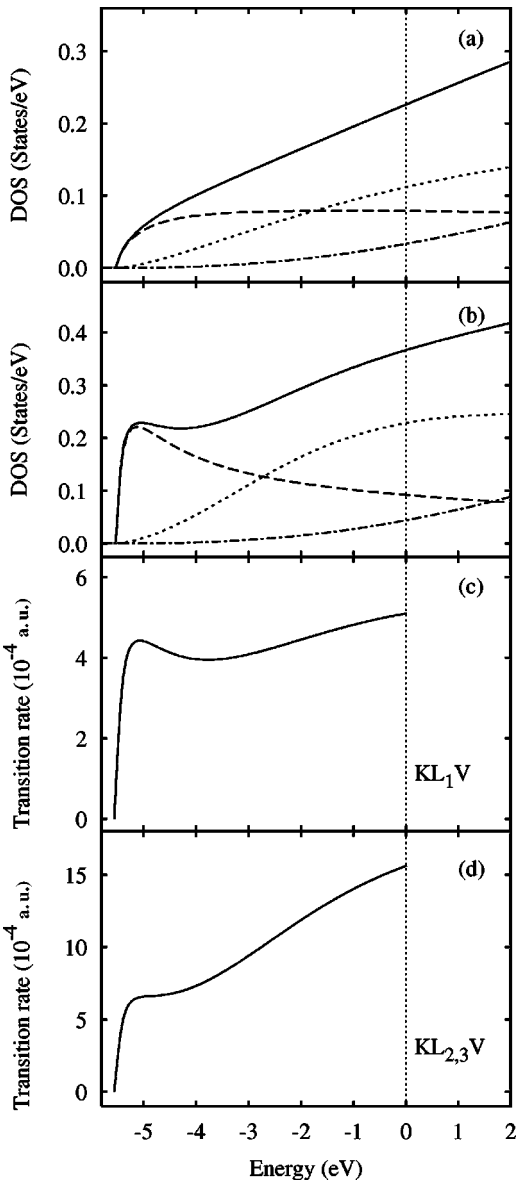

FIG. 1. Na in Ag jelliumlike bulk: (a) (solid line) the LDOS of the ground state, (b) (solid line) the LDOS of the core-ionized impurity (*s*, *p*, and *d* valence states are shown by dashed, dotted, and dash-dotted lines, respectively), (c) the KL_1V Auger transition rate, and (d) the $KL_{2,3}V$ Auger transition rate. The dotted vertical line is the Fermi level. The LDOS's are evaluated inside the Wigner-Seitz sphere ($r_s=3.02a_0$).

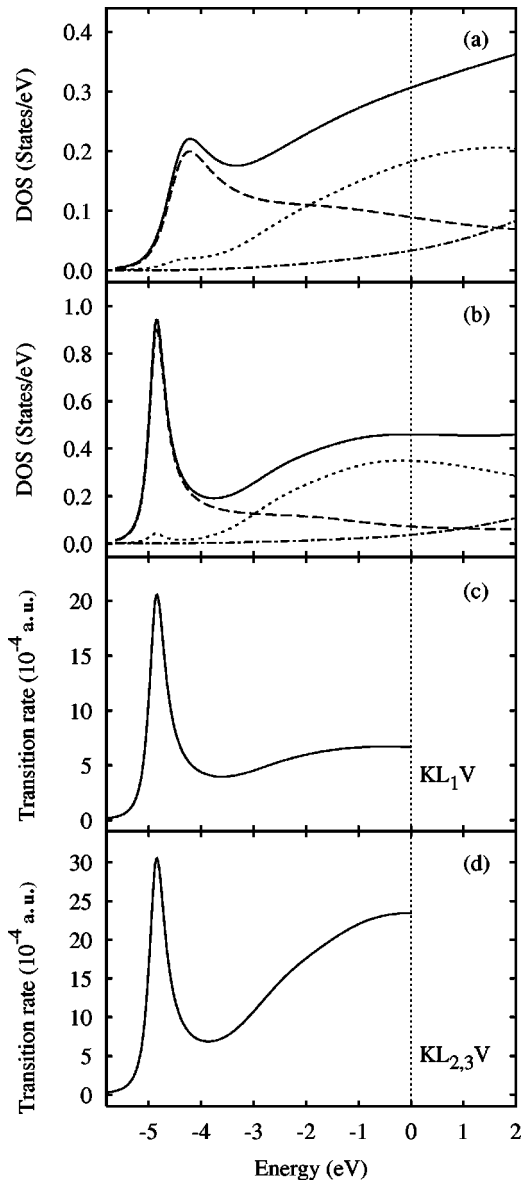

FIG. 2. The same as in Fig. 1 but for Na at $z=-2.0a_0$.

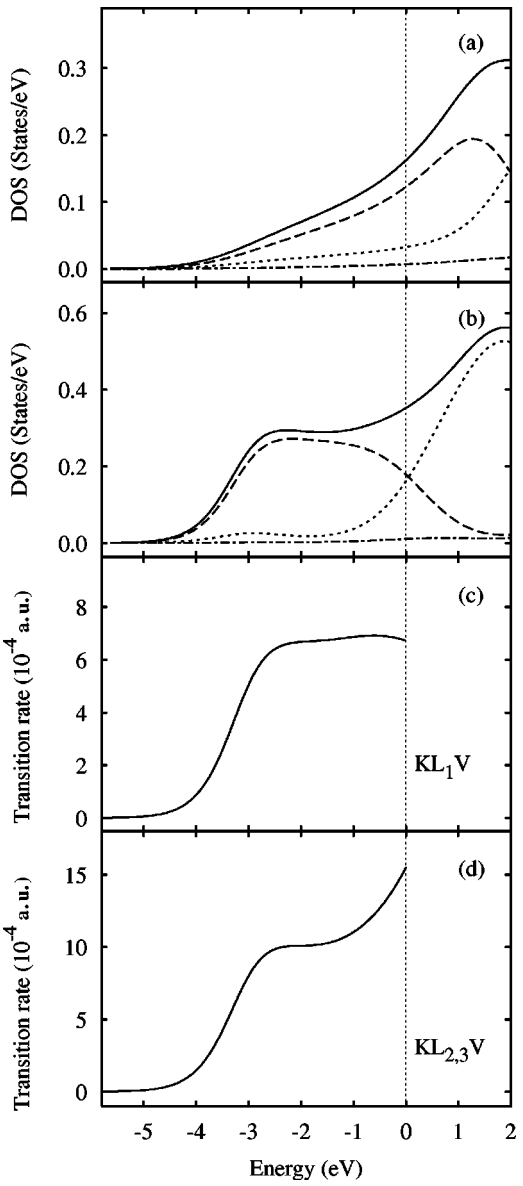

FIG. 3. The same as in Fig. 2 but for Na at $z=2.5a_0$.

tially that which screens the core hole. Though with different matrix element effects, the KL_1V and $KL_{2,3}V$ Auger transition rates [Figs. 3(c) and 3(d)] closely reflect the profile of the LDOS around the core ionized chemisorbed atom. A comparison among the Auger transition rates in Figs. 1, 2, and 3 shows that the low-energy peak shifts towards the top of the emission band as the atom is moved from bulk to surface. This is a consequence of the shift of the energy positions of the valence resonances [see LDOS's in Figs. 1(b), 2(b), and 3(b)] that tend to follow the bare-metal surface potential which increases as the atom moves from bulk to surface.[26]

In Figs. 4 and 5 we report KL_1V and $KL_{2,3}V$ Auger emission spectra obtained by convoluting the calculated transition rates with a Lorentzian of widths 0.75 and 0.42 eV, respectively.[16] As explained in Ref. 16, each width accounts for the finite lifetime of the core hole and for instrumental broadening. Inspection of the spectra in Figs. 4 and 5 demonstrates the different characteristic features of the Auger profiles according to the location of the atom with respect to the host. For example, a Na atom just inside the Ag surface shows Auger line shapes more structured than those of the same atom in bulk, displaying two well-defined peaks in the band. On the other hand, when the atom is moved outside the solid, the Auger emission band presents again a single peak which is, however, narrower than that of the same impurity in bulk.

IV. CONCLUSIONS

In this paper we have presented a full *ab initio* DFT calculation of the Auger line shapes of atomic impurities inside a metal bulk and both just inside the solid surface and chemisorbed on it. Our results show different characteristic features of the spectra according to the location of the atom with respect to the host. Such specific features could help

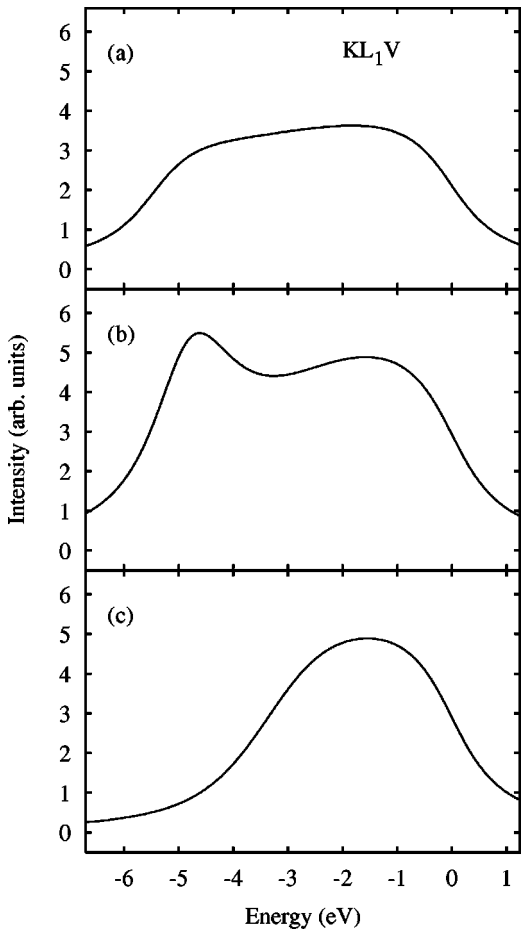

FIG. 4. KL_1V Auger profiles for (a) Na in Ag bulk, (b) Na at $z=-2.0a_0$, and (c) Na at $z=2.5a_0$. These spectral profiles are obtained by convoluting the results in Figs. 1, 2, and 3 as discussed in the text.

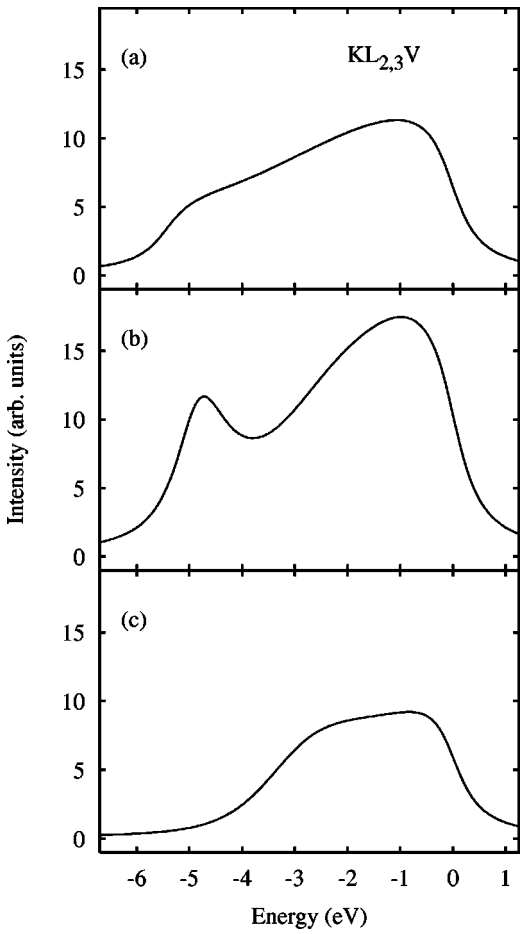

FIG. 5. The same as in Fig. 4 but for $KL_{2,3}V$ Auger profiles.

identifying different contributions to the measured Auger signal due to atoms near the surface. Besides, due to the sensitivity of Auger profiles to the local chemical environment, the investigation of Auger transitions of adatoms can provide important information about the adsorbate-substrate bond.

We wish to point out that our DFT formalism is surface specific so that our self-consistent results are not adapted from a bulk calculation where surface properties may be included within a linear-response theory framework. Also the Green-function method that we use is most suited to treat surface phenomena where continuous spectra are to be calculated such as for spectroscopic data. And for excited-state properties the jellium model is a good enough approximation for the metal substrate. Of course in general the LDA has to be implemented to include correlation effects, which are much more relevant if one deals with Auger CVV transitions than with the CCV ones treated in this paper. Another field of possible application of our method is Auger neutralization of He^+ ions[27,28] in order to study both the charge transfer and the spectra of the emitted electrons in a consistent surface approach.

[1] P. Weightman, Rep. Prog. Phys. **45**, 753 (1982).
[2] M. Thompson, M. D. Baker, A. Christie, and J. F. Tyson, *Auger Electron Spectroscopy* (John Wiley & Sons, New York, 1985).
[3] R. Lässer and J. C. Fuggle, Phys. Rev. B **22**, 2637 (1980).
[4] U. von Barth and G. Grossmann, Phys. Scr. **28**, 107 (1983).
[5] P. S. Fowles, J. E. Inglesfield, and P. Weightman, J. Phys.: Condens. Matter **3**, 641 (1991).
[6] M. Davies, P. Weightman, and D. R. Jennison, Phys. Rev. B **29**, 5318 (1984).
[7] P. H. Hannah, P. Weightman, and P. T. Andrews, Phys. Rev. B **31**, 6238 (1985).
[8] M. Davies and P. Weightman, Phys. Rev. B **30**, 4183 (1984); **32**, 8423(E) (1985).
[9] P. S. Fowles, J. E. Inglesfield, and P. Weightman, J. Phys.: Condens. Matter **4**, 8729 (1992).
[10] H. W. Haak, G. A. Sawatzky, and T. D. Thomas, Phys. Rev. Lett. **41**, 1825 (1978).

[11] R. A. Bartynsky, E. Jensen, S. L. Hulbert, and C.-C. Kao, Prog. Surf. Sci. **53**, 155 (1996).
[12] P. J. Feibelman and E. J. McGuire, Phys. Rev. B **17**, 690 (1978).
[13] C. -O. Almbladh and A. L. Morales, Phys. Rev. B **39**, 3503 (1989).
[14] J. Yuan, L. Fritsche, and J. Noffke, Phys. Rev. B **56**, 9942 (1997).
[15] B. Lohmann, S. Fritsche, and F. P. Larkins, J. Phys. B **29**, 1191 (1996).
[16] P. J. Feibelman and E. J. McGuire, Phys. Rev. B **15**, 3006 (1977).
[17] O. Gunnarsson and K. Schönhammer, Phys. Rev. B **22**, 3710 (1980).
[18] J. E. Inglesfield, J. Phys. C **14**, 3795 (1981).
[19] M. I. Trioni, G. P. Brivio, S. Crampin, and J. E. Inglesfield, Phys. Rev. B **53**, 8052 (1996).
[20] M. I. Trioni, S. Marcotulio, G. Santoro, V. Bortolani, G. Palumbo, and G. P. Brivio, Phys. Rev. B **58**, 11 043 (1998).
[21] D. E. Ramaker, Phys. Rev. B **25**, 7341 (1982).
[22] D. J. Singh, *Planewaves, Pseudopotentials and the LAPW Method* (Kluwer Academic Publishers, London, 1994).
[23] E. N. Economou, *Green's Functions in Quantum Physics* (Springer-Verlag, Berlin, 1979).
[24] G. A. Benesh and L. S. G. Liyanage, Phys. Rev. B **49**, 17 264 (1994).
[25] D. M. Ceperley and B. J. Alder, Phys. Rev. Lett. **45**, 566 (1980).
[26] N. D. Lang and A. R. Williams, Phys. Rev. B **18**, 616 (1978).
[27] M. A. Cazalilla, N. Lorente, R. Diez Muino, J. -P. Gauyacq, D. Teillet-Billy, and P. M. Echenique, Phys. Rev. B **58**, 13 991 (1998).
[28] N. Lorente, M. A. Cazalilla, J. -P. Gauyacq, D. Teillet-Billy, and P. M. Echenique, Surf. Sci. **411**, 888 (1998).